Macromolecules **1994,** *27,* 3103-3106

Notes

Stability of the OBDD Structure for Diblock Copolymer Melts in the Strong Segregation Limit

Alexey E. Likhtman and Alexander N. Semenov*

Physics Department, Moscow State University,
Moscow 117234, Russia

Received October 13, 1993

Block copolymers attract considerable interest of scientists, in particular due to their ability to form spatially periodic superstructures.[1] The symmetry (morphology) of a stable superstructure is governed primarily by the copolymer composition, f. Three fundamental morphologies (lamellar, cylindrical, and spherical) were recently supplemented by a new one, called ordered bicontinuous double diamond (OBDD).[2-7] The OBDD structure was observed in a narrow composition window between lamellar and cylindrical morphologies. The OBDD phase was also analyzed theoretically,[4] using the method of Ohta and Kawasaki.[8] However the OBDD structure was shown[4] to be less favorable than other structures for any composition.

The aim of the present contribution is just to confirm this prediction for linear diblocks in the strong segregation limit (SSL) using a more accurate approach. In fact the main conclusion (that the OBDD phase is never the most stable) is rigorous with the only reservation that interdomain boundaries belong to the family of constant-mean-curvature (area minimizing) surfaces.[9]

We use the standard model of diblock copolymers:[10,11] each chain consists of $N = N_A + N_B$ links, $f = N_A/N$ being the (mean) volume fraction of A links. It is assumed that A and B links are similar geometrically, v is the volume per link, and $6Na^2$ is the mean end-to-end distance of an unperturbed (Gaussian) copolymer chain.

We compare the three most possible structures for $f > 0.2$: lamellar, cylindrical, and OBDD. In the latter phase the minor (A) component fills two interwoven 3d periodic tetrapod networks (see Figure 1) of diamond symmetry, and the B component, the surrounding matrix. The interfaces between the A and B domains in all cases are assumed to be of constant mean curvature (see ref 4 for more details).

In the SSL considered here, which corresponds to $\chi N \gg 10$, the interfaces between the A and B domains are much thinner[10] than the characteristic period of superstructure. The excess free energy of a diblock copolymer phase in SSL can be generally represented as[12]

$$F = F_i + F_{el} \qquad (1)$$

where

$$F_i = \gamma S \qquad (2)$$

is the energy of interfaces and F_{el} is the contribution due to elongation (elastic stretch) of blocks (nearly normal to interfaces). Here S is the total interface area, and

$$\gamma = a\chi^{1/2} \qquad (3)$$

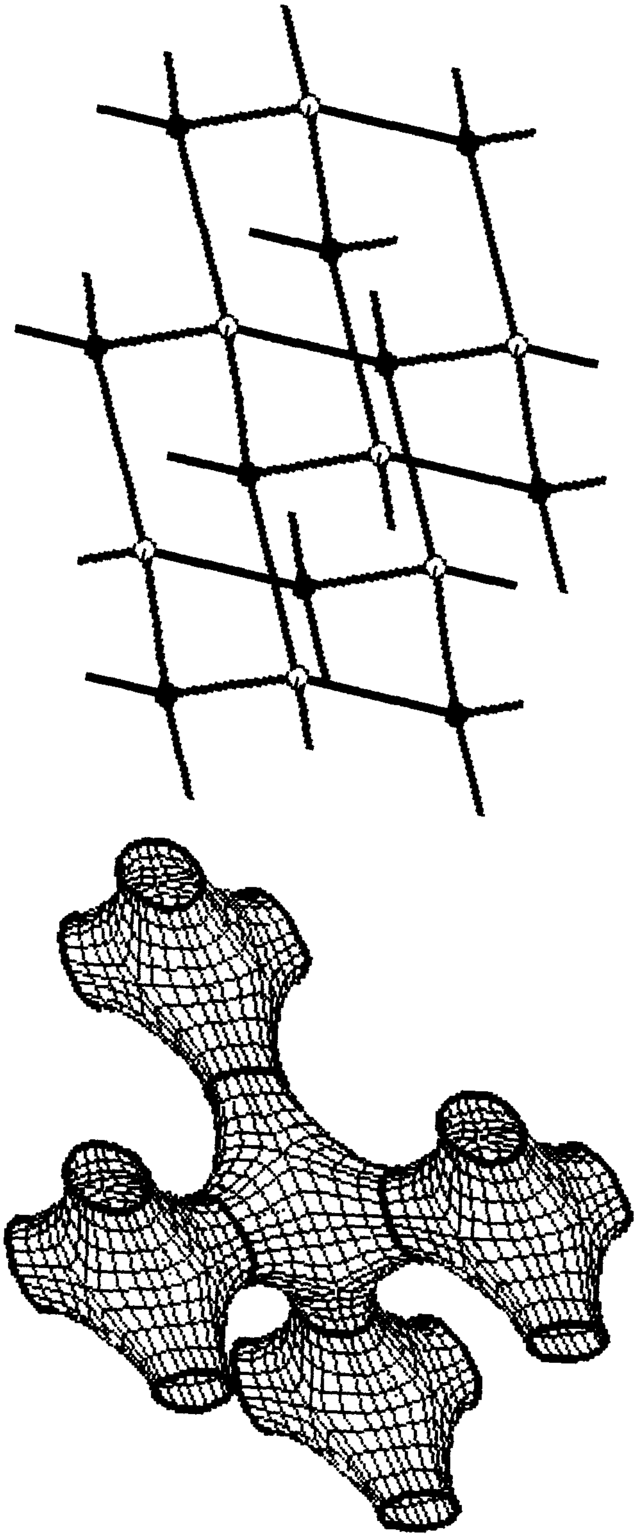

Figure 1. (a, top) Tetrapod network. (b, bottom) Structural element of the network.

is the interfacial tension[10] (here and below we take kT as a unit of energy and v as a unit of volume).

The stretch free energy F_{el} is our main concern now. Let us consider first the simplest case of the lamellar phase.

0024-9297/94/2227-3103$04.50/0

We write

$$F_{\mathrm{el}} = F_{\mathrm{el}}^{\mathrm{A}} + F_{\mathrm{el}}^{\mathrm{B}} \tag{4}$$

where $F_{\mathrm{el}}^{\mathrm{A,B}}$ are contributions due to elongation of the A and B blocks. Each of these terms is a sum of independent energies of individual chains:

$$F_{\mathrm{el}}^{\mathrm{A}}[\mathbf{r}] = \sum_{[\mathrm{A}]} \int_0^{N_\mathrm{A}} \frac{1}{4a^2} \left(\frac{\partial \mathbf{r}_n}{\partial n} \right)^2 \mathrm{d}n \tag{5}$$

and an analogous equation is valid for B blocks. Here [A] denotes all A blocks, and $\mathbf{r}_n$ is a position of the nth link of an A block ($n = 0$ corresponds to the junction point, $n = N_\mathrm{A}$ corresponds to the free end of the A block). The stretch free energy, eq 5, should be minimized for a given overall distribution of A links, $\phi(\mathbf{r}) \equiv \phi_\mathrm{A}(\mathbf{r}) = vc_\mathrm{A}(\mathbf{r})$, where $c_\mathrm{A}(\mathbf{r})$ is the local concentration of A links:[13]

$$\phi(\mathbf{r}) = \phi_\mathrm{A}(\mathbf{r}) = \begin{cases} 1, \text{ inside A domains} \\ 0, \text{ otherwise} \end{cases} \tag{6}$$

Thus

$$F_{\mathrm{el}}^{\mathrm{A}}[\phi_0] = \min_{[\mathbf{r}]:\phi(\mathbf{r})=\phi_0(\mathbf{r})} F_{\mathrm{el}}^{\mathrm{A}}[\mathbf{r}] \tag{7}$$

where $[\mathbf{r}]:\phi(\mathbf{r}) = \phi_0(\mathbf{r})$ means minimization over all possible conformations of all A blocks under the condition $\phi(\mathbf{r}) = \phi_0(\mathbf{r})$. Minimizing the right hand side of eq 7 using the Lagrange method, we write

$$F_{\mathrm{el}}^{\mathrm{A}}[\phi_0] = F_{\mathrm{el}}^{\mathrm{A}}[u] - \int u(\mathbf{r})\phi_0(\mathbf{r})\, \mathrm{d}^3\mathbf{r} \tag{8}$$

where

$$F_{\mathrm{el}}^{\mathrm{A}}[u] = \min_{[\phi]} \{F_{\mathrm{el}}^{\mathrm{A}}[\phi] + \int u(\mathbf{r})\phi(\mathbf{r})\, \mathrm{d}^3\mathbf{r}\} = \min_{[\mathbf{r}]} \{F_{\mathrm{el}}^{\mathrm{A}}[\mathbf{r}] + \sum_{[\mathrm{A}]} \int_0^{N_\mathrm{A}} u(\mathbf{r}_n)\, \mathrm{d}n\} \tag{9}$$

Minimization in eq 9 is over all possible $\phi(\mathbf{r})$; the desired profile $\phi = \phi_0(\mathbf{r})$ is now formed by the formal external field, $u(\mathbf{r})$, acting in each A link. Equation 9 can be rewritten as

$$F_{\mathrm{el}}^{\mathrm{A}}[u] = \min_{\rho} \int F_{[u]}^{\mathrm{A}}(\mathbf{R})\rho(\mathbf{R})\, \mathrm{d}^3\mathbf{R} \tag{10}$$

where $\rho(\mathbf{R})$ is the density distribution for positions ($\mathbf{R}$) of the free ends of A blocks and $F_{[u]}^{\mathrm{A}}(\mathbf{R})$ is the free energy of an A block influenced by the field $u(\mathbf{r})$ with a given position ($\mathbf{R}$) of its free end.

The minimization in eq 10, which obviously must be performed under the condition

$$\int \rho(\mathbf{R})\, \mathrm{d}^3\mathbf{R} = \langle \text{total no. of A blocks} \rangle$$

leads to the equation

$$F_{[u]}^{\mathrm{A}}(\mathbf{R}) = \text{constant} \tag{11}$$

for any $\mathbf{R}$ inside the A domains.

Now let us recall that we are considering a 1 d lamellar structure, so that $u = u(z)$, where $z = z(\mathbf{r})$ is the distance from a given point ($\mathbf{r}$) to the nearest interface. The only solution (for a 1d structure) of eq 11 (which is equivalent to the so-called equal time constraint[14]) is the parabolic field profile:[12,14]

$$u(z) = -\frac{1}{2}\alpha z^2 \tag{12}$$

where α depends on the length of the A blocks:

$$\alpha = \frac{\pi^2}{8} \frac{1}{{N_\mathrm{A}}^2 a^2} \tag{13}$$

It is easy to show that with eq 12 the constant in the right hand side of eq 11 should be equal to zero:

$$F_{[u]}^{\mathrm{A}}(\mathbf{R}) = 0 \tag{14}$$

Using eqs 8, 10, and 12–14 we thus get

$$F_{\mathrm{el}}^{\mathrm{A}} = \frac{\pi^2}{16} \frac{1}{{N_\mathrm{A}}^2 a^2} \int_{[\mathrm{A}]} z^2(\mathbf{r})\, \mathrm{d}^3\mathbf{r} \tag{15}$$

where the integration is performed over the volume of all A domains.

Let us return to the general case of arbitrary (nonlamellar) structure and curved interfaces. A reconsideration of the derivation of eq 15 presented above shows that actually we do not need an assumption that interfaces are plain. Thus it looks as if eq 15 is valid in the general case if $z(\mathbf{r})$ is defined as the shortest distance from a given point to the nearest interface. In fact one can easily check that eq 15 works precisely for lamellar sheets and spherical and cylindrical domains (inner parts; compare with results of ref 12).

If we try to use eq 15 to predict the elastic energy of the outer part of, e.g., a cylinder (i.e. a brush grafted to the outside of a cylinder), one complication would arise. In this case a parabolic potential (eq 12) will formally imply the end density distribution $\rho(\mathbf{R})$ which must be negative in a narrow zone near the cylinder.[12,15] Thus with the additional physical condition

$$\rho(z) \geq 0$$

the formal minimum (eq 15) cannot be achieved, so that the true elastic free energy must be higher: it should correspond to the real end distribution which must be exactly equal to zero in a narrow excluded zone near the cylinder (the interface).[15] Therefore, in this case eq 15 provides a lower boundary for the elastic stretch free energy.

The relative difference between the true elastic energy and eq 15 depends on the interface curvature. For small curvatures this difference is exponentially small.[15] Moreover, using the result of ref 15, we managed to show that in the composition region of interest ($f \gtrsim 0.3$)[16] the relative error of eq 15 should be less than 0.06%. We shall see that this error is surely negligible for our main conclusions. Thus eq 15 can be used for elastic free energies of lamellar, cylindrical, and OBDD phases.

Using eqs 1–4 and 15 we write the free energy per copolymer chain as

$$F = Na\chi^{1/2}\frac{S_0}{V_0} + \frac{\pi^2}{16}\frac{1}{Na^2V_0}\left\{\frac{1}{f^2}\int_{[\mathrm{A}]} z^2(r)\, \mathrm{d}^3r + \frac{1}{(1-f)^2}\int_{[\mathrm{B}]} z^2(r)\, \mathrm{d}^3r\right\} \tag{16}$$

where V_0 is the volume of a Wigner–Seitz cell (Figure 2), S_0 is the interfacial area per cell, and [A] and [B] denote the corresponding parts of a cell.

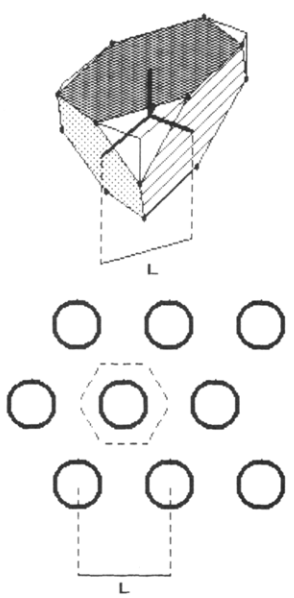

Figure 2. Wigner-Seitz cell (a, left) for an OBDD structure and (b, right) for a cylindrical structure.

For a given morphology the free energy, F, should be minimized over the "period" L (see Figure 2). The result is

$$F = (\chi N)^{1/3}\tilde{F}(f) \tag{17}$$

where $\tilde{F}(f)$ is a numerical factor:

$$\tilde{F}(f) = \frac{3}{2^{2/3}}\left\{\frac{\pi^2}{16}\frac{{S_0}^2}{{V_0}^3}\left[\frac{1}{f^2}\int_{[A]} z^2(r)\,\mathrm{d}^3r + \frac{1}{(1-f)^2}\int_{[A]} z^2(r)\,\mathrm{d}^3r\right]\right\}^{1/3} \tag{18}$$

the equilibrium period being

$$L = N^{1/2}a(\chi N)^{1/6}\tilde{L}(f) \tag{19}$$

where $\tilde{L}(f)$ is another numerical factor.

For both lamellar and cylindrical phases the free energies can be calculated analytically:

$$\tilde{F}_{\mathrm{lam}}(f) = \frac{3}{2^{2/3}}\left(\frac{\pi^2}{48}\right)^{1/3} \tag{20}$$

$$\tilde{F}_{\mathrm{cyl}}(f) = \frac{3}{2^{2/3}}\left\{\frac{\pi^3 f}{18}\left[\frac{3}{16\pi} + 2\left(\frac{5}{32\sqrt{3}} - \frac{3}{4}\sqrt{\frac{3^{1/2}f}{2\pi}}\left(\frac{1}{3} + \frac{1}{4}\ln 3\right) + \frac{9f}{16\pi} - \frac{3f^2}{32\pi}\right)\right]\right\}^{1/3} \tag{21}$$

The last two equations imply that (if we forget about a possibility of OBDD and other nontrivial morphologies) the transition from lamellar to cylindrical structure should occur at

$$f = 0.293 \tag{22}$$

This value agrees well with slightly less accurate previous results.[12,17]

In order to calculate the free energy of the OBDD phase, we have first to calculate an area minimizing interface within a Wigner–Seitz cell for a chosen composition f. In fact, only 1/24*th* of the cell should be considered (as it can be divided into 24 congruent parts). An area minimizing surface was calculated using an analogy with a "soap film" filled by an ideal gas. Different compositions can be achieved by changing the "external" pressure in the B matrix. The "minimal" Schwarz surface[4] which divides "regions of influence" of two tetrapod networks in our model corresponds to the case of equal pressure inside and outside the soap film (inside the A network and B matrix). The calculated area of the Schwarz surface coincides with the exact value within an error less than 0.03%.

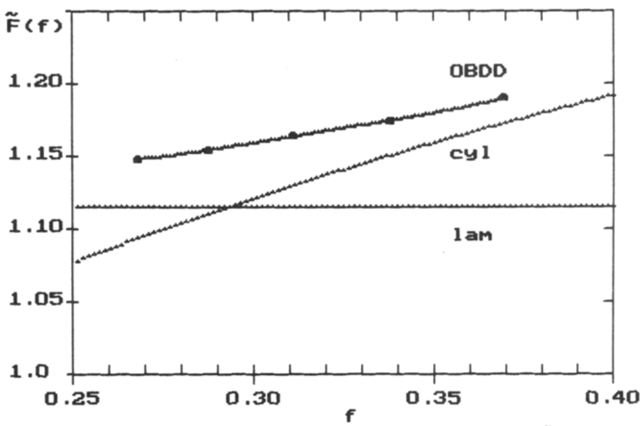

Figure 3. Dependence of the reduced free energy, $\tilde{F}$, on the composition, f, for lamellar, OBDD, and cylindrical phases.

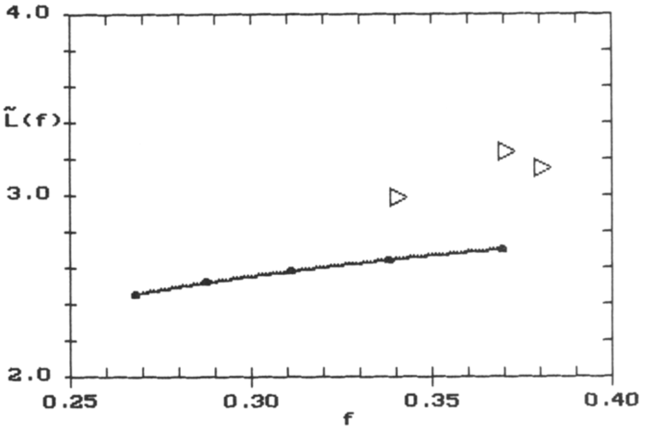

Figure 4. Dependence of the reduced period, $L = L/(N^{2/3}a\chi^{1/6})$ (where L is the lattice parameter of the OBDD phase), on composition: (triangles) experimental data of ref 6.

Using the family of interfaces thus calculated and eq 16, we obtain the reduced free energies of OBDD structures in the composition range $f = 0.27$–0.37, where lamellar and cylindrical structures compete with each other. The final error was estimated to be less than 0.2%. Composition dependence of the reduced free energies, $\tilde{F}$, for lamellar, cylindrical, and OBDD structures are plotted in Figure 3; the same dependence for the reduced lattice parameter, $\tilde{L}$, of the OBDD is shown in Figure 4. Experimental data[6] for $\tilde{L}$ are also shown in Figure 4.

An examination of Figure 3 shows that the OBDD structure is never stable in the compositional range of interest: its free energy is always larger than that of cylindrical or lamellar phases by about 4% or more. Note that this difference is much larger than a possible theoretical error (due to both model assumption and numerical approximation).

We may conclude that the experimentally observed OBDD phase is probably metastable, its formation being governed by dynamic effects. It is worth generalizing the calculations in order to take into account the possible geometrical asymmetry of the A and B links. An analysis of OBDD-like structures in copolymer/homopolymer blends is also of interest.

Acknowledgment. This work was supported, in part, by a Soros Foundation Grant awarded by the American Physical Society.

References and Notes

(1) Goodman, I. *Developments in Block Copolymers*; Applied Science: New York, 1982 and 1985; Vols. 1 and 2.
(2) Thomas, E. L.; Anderson, D. M.; Henkee, C. S.; Hoffman, D. *Nature* **1988**, *334*, 598.
(3) Thomas, E. L.; Alward, D. B.; Kinning, D. J.; Martin, D. S.; Handlin, D. L., Jr.; Fetters, L. J. *Macromolecules* **1986**, *19*, 2197.
(4) Anderson, D. M.; Thomas, E. L. *Macromolecules* **1988**, *21*, 3221.
(5) Alward, D. B.; Kinning, D. J.; Thomas, E. L.; Fetters, L. J. *Macromolecules* **1986**, *19*, 215.
(6) Hasegawa, H.; Tanaka, H.; Yamasaki, K.; Hashimoto, T. *Macromolecules* **1987**, *20*, 1651.
(7) Winey, K. I.; Thomas, E. L.; Fetters, L. J. *Macromolecules* **1992**, *25*, 442.
(8) Ohta, T.; Kawasaki, K. *Macromolecules* **1986**, *19*, 2621.
(9) This assumption was strongly supported by analysis of ref 4.
(10) Helfand, E.; Wasserman, Z. R. *Macromolecules* **1976**, *9*, 879.
(11) Leibler, L. *Macromolecules* **1980**, *13*, 1602.
(12) Semenov, A. N. *Sov. Phys. JETP* **1985**, *61*, 733.
(13) Note that junction points are effectively attached to the interfaces with a 2d density, which is determined by the period of lamellar structure.
(14) Milner, S. T.; Witten, T. A.; Cates, M. E. *Macromolecules* **1988**, *21*, 2610.
(15) Ball, R. C.; Marko, J. F.; Milner, S. T.; Witten, T. A. *Macromolecules* **1991**, *24*, 693.
(16) Note that experimentally observed OBDD window is normally within the region $f > 0.3$; the same is true for the composition corresponding to the transition between cylindrical and lamellar morphologies as predicted by theories.
(17) Semenov, A. N. *Macromolecules* **1993**, *26*, 2273.